Expanded View Figures

Figure EV1. Colocalization of Siwi-D670A, BmSpnE, BmQin in P-bodies.

A Colocalization of Siwi-D670A with BmSpnE or BmQin in non-perinuclear cytoplasmic condensates. Scale bar 8 μm.

B Colocalization of wild-type piRNA factors with BmDcp2 in P-bodies. BmSpnE and BmQin, but not BmVasa, are localized in BmDcp2-containing P-bodies. Scale bar 8 μm.

C Localization of Siwi piRNA loading mutant (Y607E) in BmN4 cells. (Top) Siwi-Y607E is largely dispersed in the cytoplasm. (Bottom) Introduction of Y607E mutation into Siwi-D670A compromised its colocalization with BmDcp2. Scale bar 8 μm.

D Colocalization of endogenous BmMael with BmDcp2, Siwi, and Siwi-D670A. BmMael is partially localized to the peripheral region of BmDcp2-containing P-bodies and is strongly colocalized with both wild-type and mutant Siwi in nuage and P-bodies, respectively. Scale bar 10 μm (cell), 2 μm (foci, enlarged region from the white box).

E Colocalization of stably expressed GFP-BmArmi with Siwi and Siwi-D670A. BmArmi is partially localized to both Siwi (nuage) and Siwi-D670A (P-bodies). Scale bar 10 μm (cell), 2 μm (foci, enlarged region from the white box).

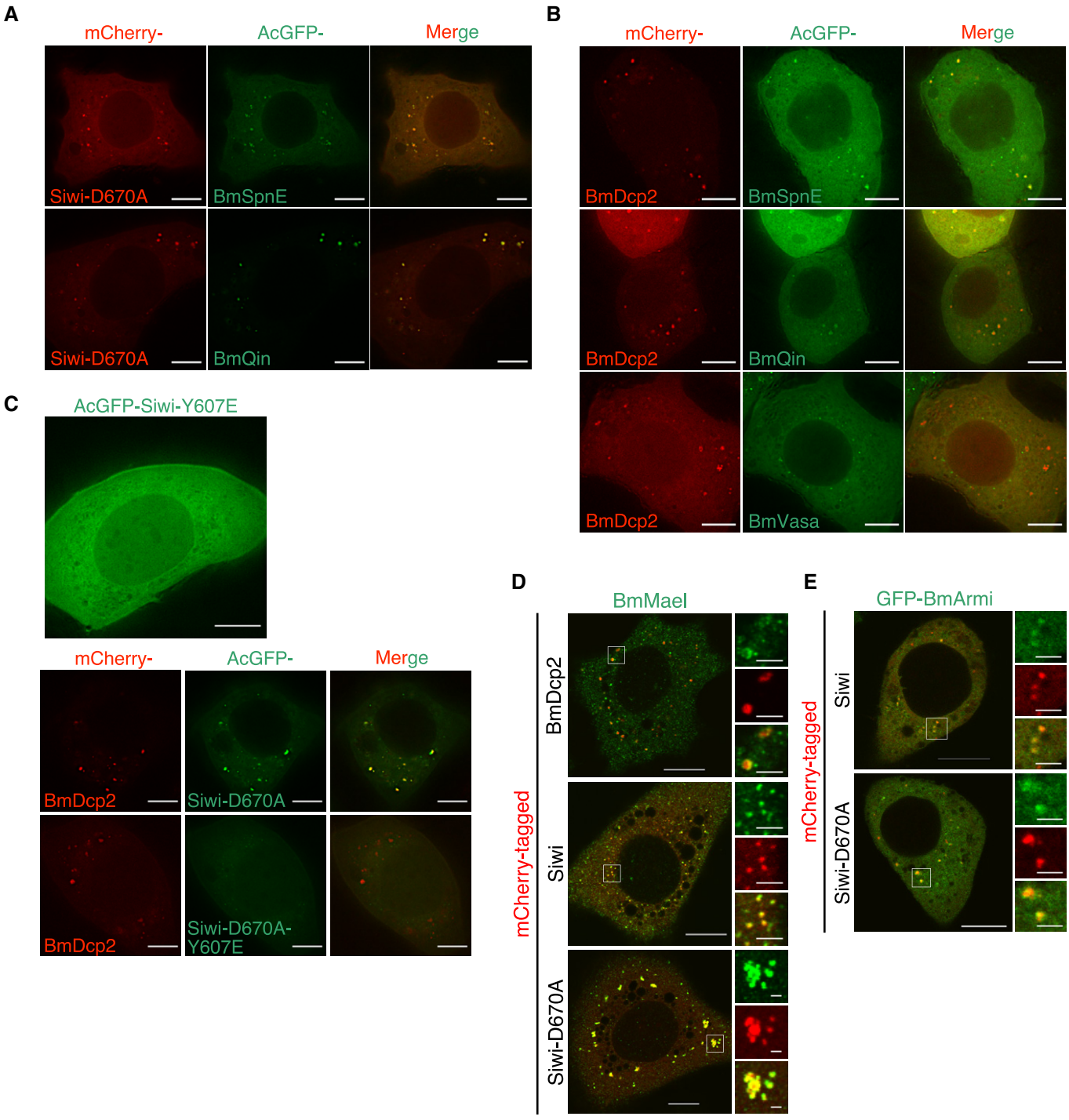

Figure EV1.

Figure EV2. Reduction in protein expression level with Tet-On inducible promoter.

A Western blotting of endogenous counterparts and the epitope-tagged version of the protein-of-interest (POI), either expressed by an OpIE2 promoter (pIZ) or a Tet-On system (pTet). Most of the pIZ constructs express epitope-tagged POI (upper bands) at levels comparable to the endogenous counterparts (lower bands) and all of the pTet constructs express POI at significantly lower levels than the pIZ constructs and the endogenous counterparts.

B Relative whole-cell fluorescence intensity of AcGFP-tagged POI expressed by an OpIE2 promoter (pIZ) or a Tet-On system (pTet).

C Flow cytometry analysis of pIZ-AcGFP-Siwi or pTet-AcGFP-Siwi transfected cells. Naive BmN4 was used as a negative control (0.18% GFP-positive cells (GFPpos); See Appendix Figure S1). pIZ construct yielded 8.45% GFPpos, while pTet yielded 2.5% GFPpos that were roughly 30–100 folds dimmer than pIZ-GFPpos. FSC: Forward scatter. For the gating strategy, see Appendix Figure S1.

D Colocalizations of Siwi-D670A, BmSpnE, and BmQin with BmDcp2, or BmVasa-E339Q with Siwi-D670A were not affected by the reducing POI expression level with pTet. Scale bar 10 μm.

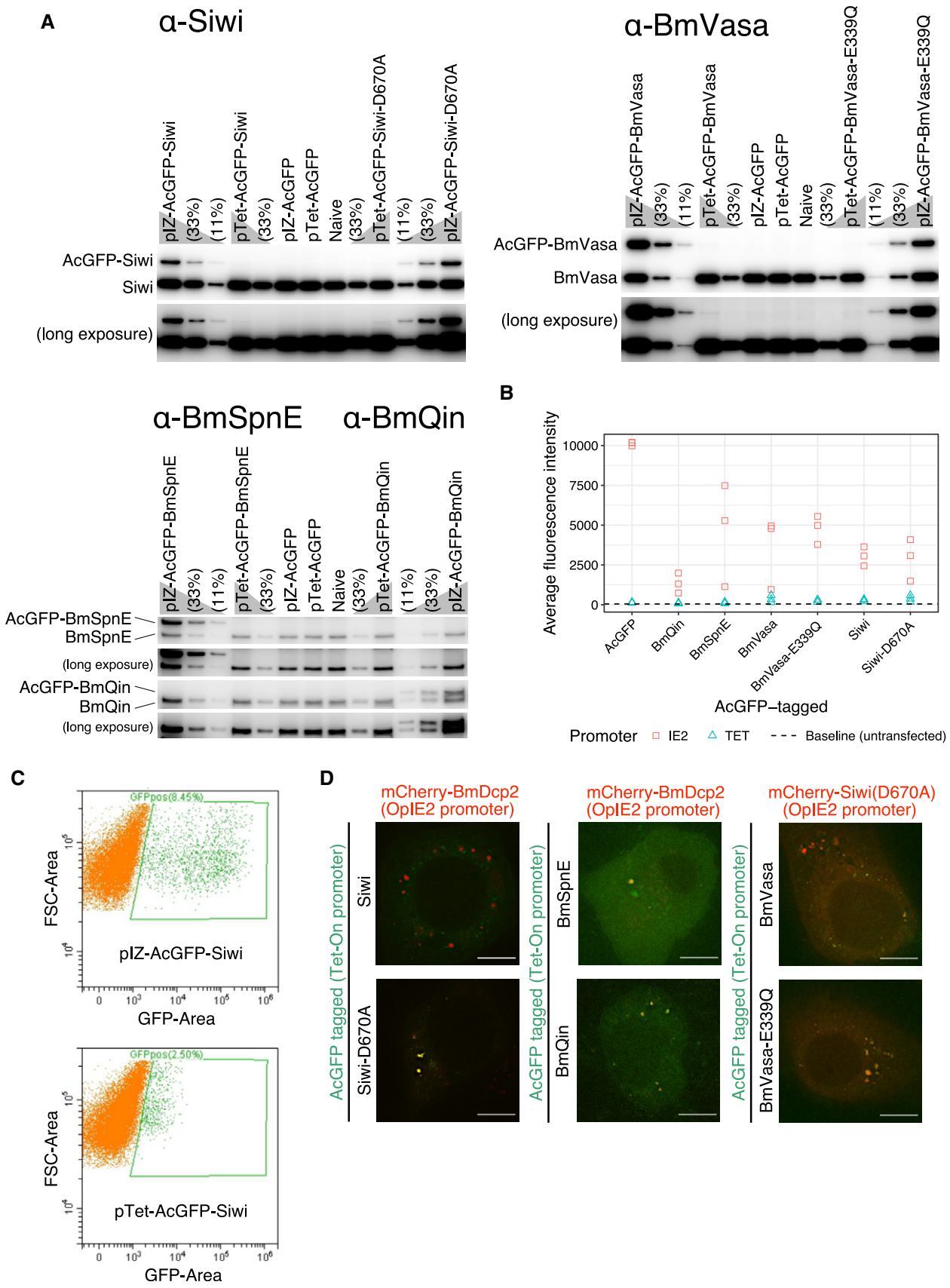

Figure EV2.

Figure EV3. Validation of dsRNA-mediated knockdown of piRNA factors, effects of BmMael knockdown, and BmVasa ATPase mutation.

A Western blotting of AcGFP-Siwi, wild-type (WT) or D670A, and the co-expressed mCherry-BmQin or mCherry-BmSpnE. Expression of Siwi-D670A did not affect the expression level of BmQin or BmSpnE.

B Validation of dsRNA-mediated knockdown of epitope-tagged piRNA factors by Western blotting.

C Validation of dsRNA-mediated knockdown of endogenous piRNA factors by Western blotting.

D Depletion of BmMael results in partial segregation of Siwi-D670A foci from BmDcp2 foci. (Top-left) Representative Z-projections (Maximum intensity). Scale bar 8 μm. (Top-right) Enlarged area from the white box. Scale bar 2 μm. (Bottom) Box plot showing that depletion of BmMael (dsBmMael, $n = 24$ cells) reduced colocalization ratio between Siwi and BmDcp2, compared with control (dsRLuc, $n = 24$ cells). Representative data from $N = 3$ independent experiments are shown. *P*-value was calculated by asymptotic Wilcoxon rank sum test. Centre line, median; box limits, lower (Q1), and upper (Q3) quartiles; whiskers, 1.5 × interquartile range (IQR); points, outliers.

E Colocalization of BmAgo3 and BmQin with BmVasa-E339Q (ATPase mutant). Scale bar 10 μm.

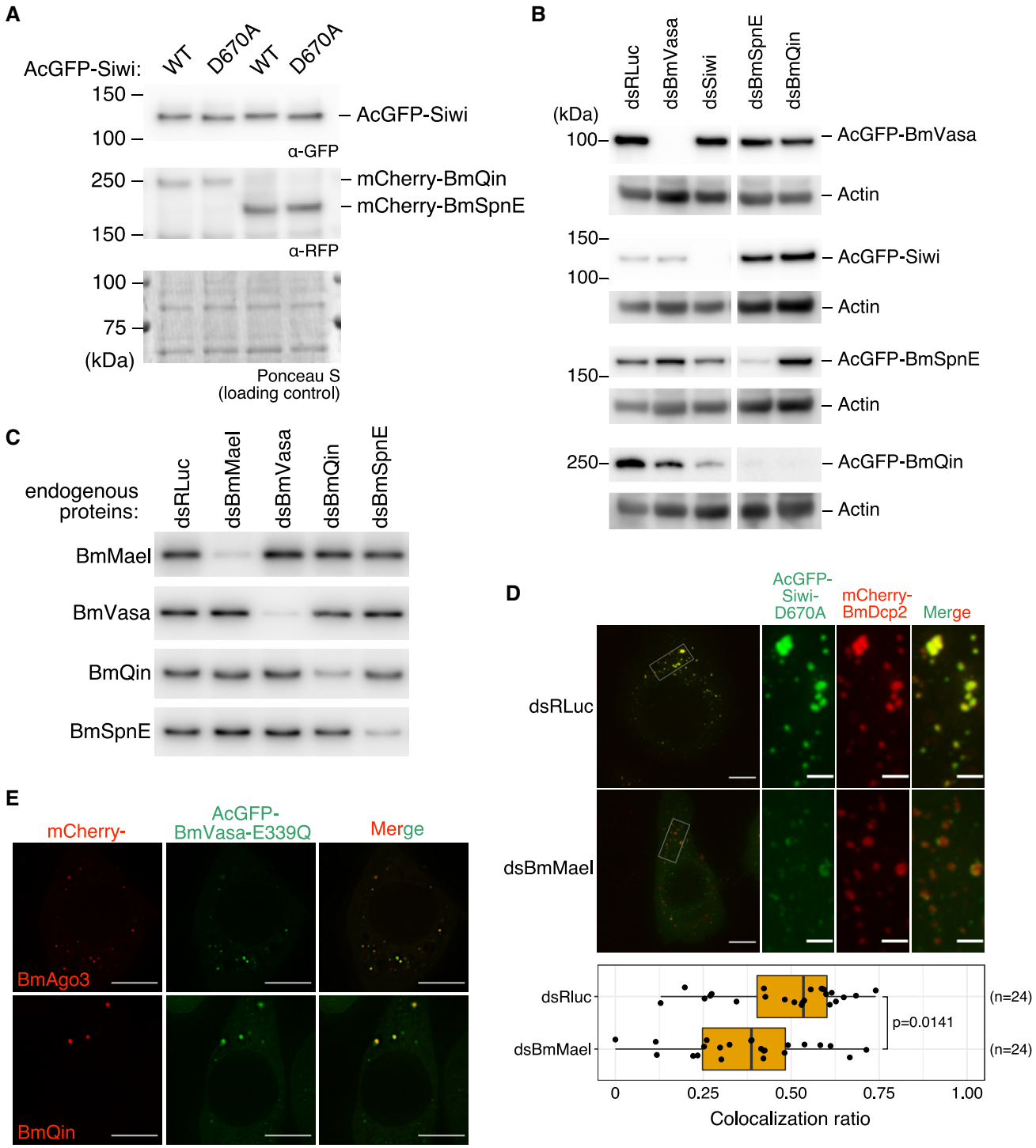

Figure EV3.

Figure EV4. Definition of potential-TE genes and analysis of piRNA hallmarks.

A MA plot of differential piRNA expression analysis between two naive small RNA libraries. Reads longer than 25-nt are mapped to predicted genes (Silkbase GeneModel) that do not have a BLAST (tblastx) hit with known transposons (Silkbase Transposon Database). Mean piRNA expression with an RPM higher than 2^4 is defined as potential TE-derived piRNAs (potential TEs).

B Length distribution of piRNA reads mapped to different groups of predicted genes. Peak length of piRNAs mapped to TEs and potential TEs are both 27-nt, while peak length of piRNAs mapped to non-TEs is 28-nt. Note that despite that Siwi-D670A causes significant upregulation of 28-nt piRNA from non-TEs, the expression of siRNA/miRNA at 20-nt peak remains unchanged between Siwi and Siwi-D670A libraries.

C Nucleotide bias of the 1st and 10th nucleotide of non-TE-derived piRNAs in Siwi and Siwi-D670A libraries. (Top) Ratios of uracil as the 1st nucleotide of piRNAs (1 U bias) in TEs and potential TEs are roughly 80% in both libraries. In non-TEs, 1 U bias is retained at 38% in Siwi-WT library and 45% in Siwi-D670A library, which is higher than the control (the frequency of uracil in all CDSs, 23%, black dotted line), suggesting the mapped reads contain *bona fide* piRNAs. (Bottom) A bias of favoring adenine at the 10th nucleotide (10A bias) can be found in ping-pong piRNAs. 10th nucleotides of TE piRNAs (~ 44%) and potential TE piRNAs (~ 38%) are mildly biased to adenine, compared with the control frequency of adenine in all CDSs (29%, black dotted line). Non-TE-derived piRNAs do not have an apparent 10A bias (~ 30%, similar to the control), suggesting that non-TE-derived piRNAs are generated independently of the ping-pong cycle.

D Analysis of the strand directionality of mapped piRNA reads. Strand directionality is calculated by counting and dividing sense reads over antisense reads, and the mean strand directionality is calculated between the 2 naive libraries. A strand directionality of 1.0 means that only sense reads are mapped to the predicted CDS region, while −1.0 means only antisense reads are mapped. In non-TEs genes, most of the mapped piRNAs are in sense direction. In contrast, potential TEs genes are mapped with piRNA reads from both directions, suggesting the involvement of ping-pong machineries. Dashed line: expression threshold value (2^4 RPM) for the definition of potential TE genes.

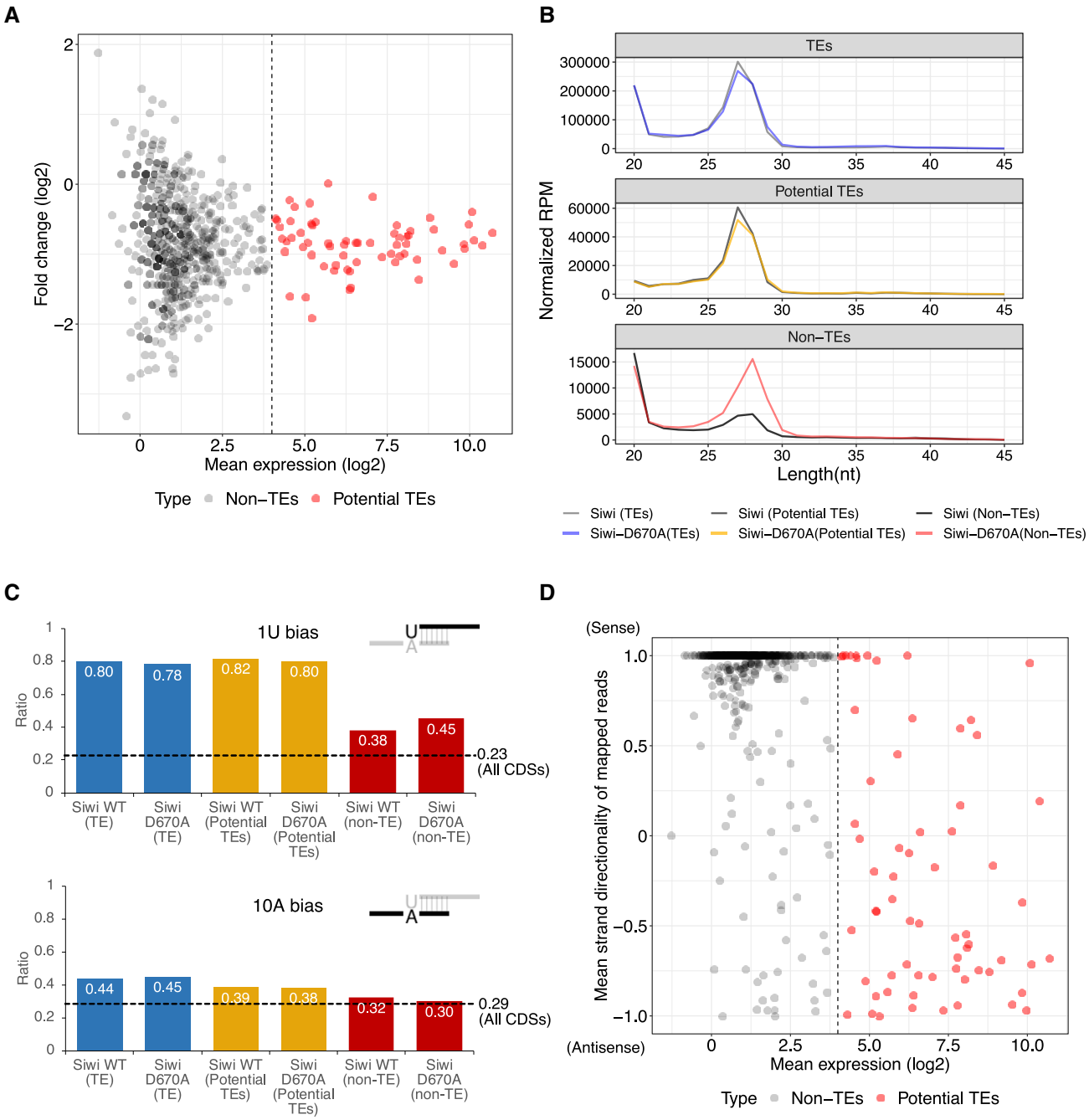

Figure EV4.

Figure EV5. Upregulated non-TE piRNAs in Siwi-D670A expressed cells are 2′-*O*-methylated.

A MA plots of differential piRNA expression analysis of Siwi/Siwi-D670A- overexpressed (OE) cells against mCherry-OE cells. Reads longer than 25-nt are mapped to predicted genes (Silkbase GeneModel) and non-TE genes derived reads are upregulated only in Siwi-D670A-OE cells. $NaIO_4$ treatment did not deplete the upregulation.

B Split violin plots of piRNA expression fold change between mCherry (control) and Siwi (WT/D670A) overexpressed libraries with or without $NaIO_4$ treatment. Non-TE piRNAs (red, 628 genes) upregulated or TE piRNAs (blue, 811 genes) remained unchanged in Siwi-D670A-OE cells have a similar distribution and mean value regardless of $NaIO_4$ treatment. Bonferroni-corrected *P*-values and the effect sizes (*r*) were calculated by asymptotic Wilcoxon rank sum test. Box plot: Centre line, median; box limits, lower (Q1), and upper (Q3) quartiles; whiskers, 1.5 × interquartile range (IQR); points, outliers.

C MA plot of $NaIO_4$ + against $NaIO_4$ − small RNA libraries from Siwi-D670A-OE cells. A mild depletion of the less abundant piRNAs is observed similarly with TE, potential TE and non-TE piRNAs.

D Length distribution of mCherry-, Siwi-, and Siwi-D670A-OE cells (± $NaIO_4$ treatment). Two peaks (20-nt and 27-nt) correspond to siRNA/miRNA and piRNA respectively. The first peak (20-nt) is depleted after $NaIO_4$ treatment, leading to an increase of the read counts of the piRNA peak (27-nt) in those libraries.

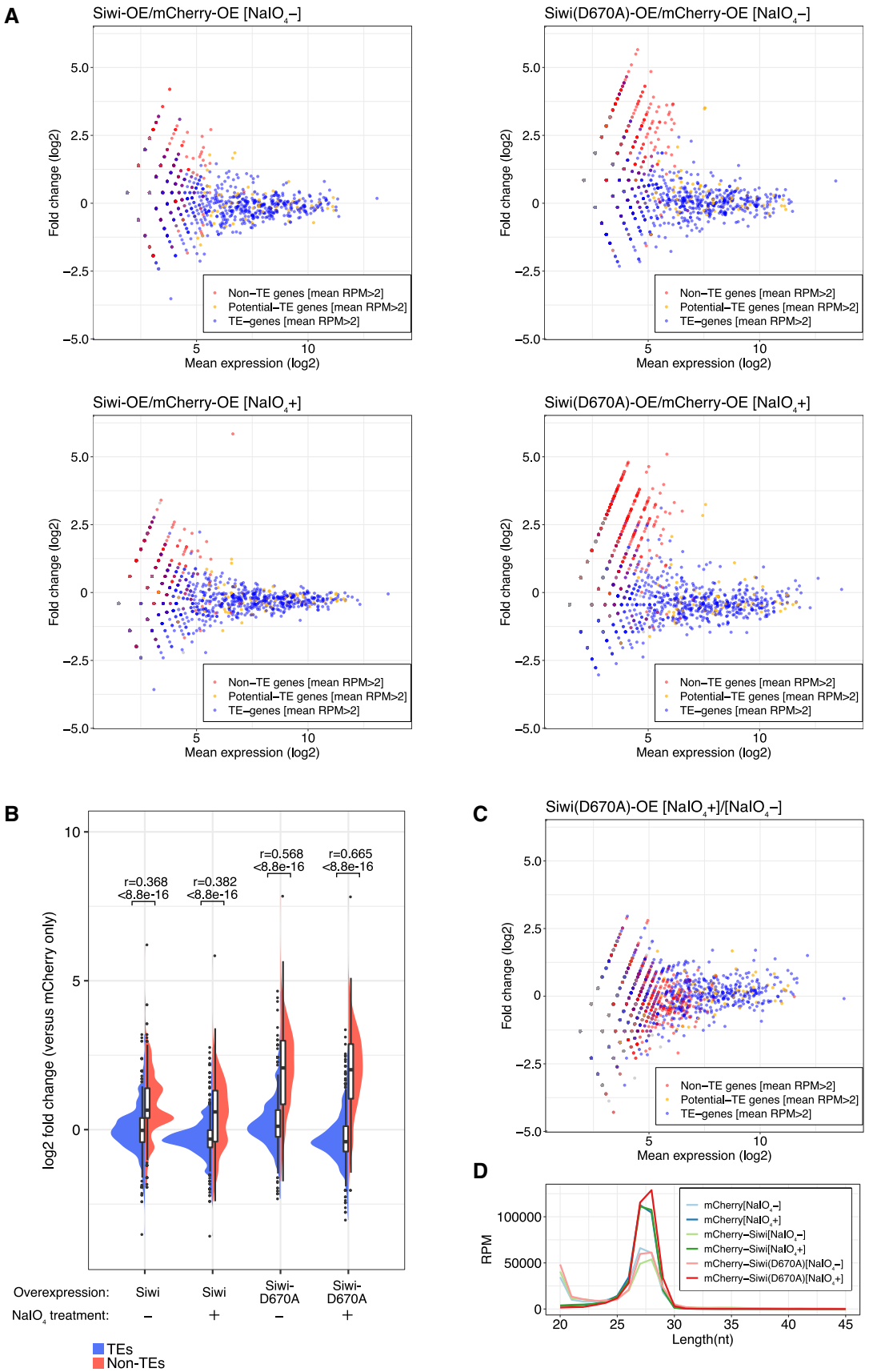

Figure EV5.